Performance of Spatially Diverse URLLC and eMBB Traffic in Cell Free Massive MIMO Environments

Ubaldo Bucci, *Student Member, IEEE*, Dajana Cassioli, *Senior Member, IEEE*, and Andrea Marotta, *Member, IEEE*

***Abstract*—5G networks are designed to support both high data rate eMBB services, and low-latency high-reliability URLLC services. Multiplexing these two services on the same wireless frequency band leads to a challenging radio resource allocation problem due to their heterogeneous requirements. Usually, multiplexing is based on the puncturing mechanism by URLLC traffic at the expense of the eMBB throughput's reduction. In this paper, we investigate the potential of cell-free massive MIMO to multiplex URLLC and eMBB traffic by exploiting the sole spatial diversity through network slicing. We define a theoretical framework to evaluate the system's performance, based on closed-form expressions for the spectral efficiency and the throughput of eMBB and URLLC services in this new asset. We show that *by design* the cell-free massive MIMO architecture can support such heterogeneous services without relying on sophisticated interference management techniques or pilot assignment schemes, while guaranteeing their specific QoS requirements.**

***Index Terms*—Cell-free, massive MIMO, URLLC, eMBB.**

I. Introduction

THE EVER-GROWING demand for heterogeneous 5G services calls for new technological solutions with enhanced flexibility, to target both capacity and scalability. The 5G radio access network (RAN) is designed to support, among others, the traffic belonging to the service class of ultra-reliable low-latency communication (URLLC), which requires immediate scheduling and transmission once it arrives at the Base Station (BS). Simultaneously, and sharing the same available wireless spectrum, the high data rate traffic of enhanced mobile broadband (eMBB) users has to be multiplexed in the 5G RAN.

Regardless of the specific service, the approach of the conventional *cellular* architecture is to allocate to users *orthogonal* radio resources, to achieve the target Quality of Service (QoS). Instead, for the specific case of eMBB and URLLC multiplexing, the Third Generation Partnership Project (3GPP) standard has proposed the *superposition/puncturing schemes* performing the immediate transmission of arriving URLLC packets in the next 0.125 ms *mini-slot* over the ongoing eMBB resources. In this context, the puncturing technique consists of puncturing a part of the frequency resources allocated to an eMBB user at the beginning of each time slot, and re-allocating this resource part to some URLLC packets [1].

The puncturing scheme preserves the reliability of URLLC transmissions, because the eMBB users originally allocated to the punctured resources are muted during URLLC transmissions. However, since the punctured resources are subtracted to the eMBB service class, the eMBB users may undergo a significant reduction of the throughput, especially in low SNR scenarios, due, e.g., to high overhead and likely retransmissions [2]. Another technique is the *superposition*, which consists of superimposing the URLLC and eMBB packets within a part of the frequency resources originally allocated to an eMBB user at the beginning of each time-slot [3]. In this case, however, the superposition may impact the reliability of URLLC packets due to the interference caused by eMBB traffic.

To facilitate the coexistence of multiple services having very different target requirements in terms of data rate and latency, the 5G ecosystem has introduced the *network slicing* (NS). NS is a breakthrough technology able to guarantee a *sustainable coexistence* of multiple heterogeneous services, while fulfilling their specific QoS requirements and maintaining a great level of flexibility in orchestrating the available resources. Furthermore, the conventional *cellular* architecture leaves the way to a new setting for the 5G RAN, which does not involve any concept of cell or cells' boundaries, i.e., it is "Cell-Free." The Cell-free Massive Multiple Input Multiple Output (Cf-maMIMO) shows a great balance of performance and flexibility [4]. Its benefits are the huge throughput, the higher coverage probability, energy efficiency, and its capability of averaging out the *small-scale fading* and uncorrelated noise, resulting in improved performance only subject to the *large-scale fading*. Cf-maMIMO is a *distributed Massive MIMO* system where a large number of antennas, named Access Points (APs), serve a much smaller number of autonomous users that share the resources according to a time-division duplex (TDD) operation mode. Compared to the conventional co-located massive MIMO schemes, cell-free networks

Manuscript received 24 July 2022; revised 21 February 2023; accepted 26 June 2023. Date of publication 1 August 2023; date of current version 7 February 2024. This work has been partially supported by the European Commission through the project H2020-MSCA-RISE-2019-872866-OPTIMIST. The associate editor coordinating the review of this article and approving it for publication was J. Hwang. *(Corresponding author: Dajana Cassioli.)*

The authors are with the Department of Information Engineering, Computer Science and Mathematics, University of L'Aquila, 67100 L'Aquila, Italy (e-mail: ubaldo.bucci@graduate.univaq.it; dajana.cassioli@univaq.it; andrea.marotta@univaq.it).

Digital Object Identifier 10.1109/TNSM.2023.3300966

offer a more uniform connectivity for all users thanks to the macro-diversity gain obtained by the distributed antennas [5].

The APs can cooperate through the fronthaul/backhaul network. Typically, this system relies on a Central Processing Unit (CPU) for the execution of the tasks ruling the entire system, like, e.g., pilot assignment procedures (PAs) and power control mechanisms. The PAs rely on accurate channel state information (CSI) available at the transmitter (or receiver). In both cellular massive MIMO and Cf-maMIMO networks, CSIs are acquired through uplink (UL) pilot transmissions during the *training phase*. The information exchange between APs and CPU results in additional fronthaul load and effective solutions are being devised to reduce this overhead. The authors in [6] proposed to quantize the transmitted signals and use structured lattice codes.

Although Cf-maMIMO has been investigated for several years, its practical deployment still entails some open challenges. Many researchers aim to incorporate into the Cf-maMIMO scheme the new enabling technologies for future wireless communications, like, e.g., the 6G [5]. However, for an ubiquitous Cf-maMIMO deployment, novel low-cost and low-complexity hardware platforms are needed, like, e.g., the *radio strip system* [7].

Several studies are available in the literature about innovative resource allocation schemes to guarantee the coexistence and multiplexing of the URLLC and eMBB traffic while fulfilling their heterogeneous requirements [8], [9], [10], [11]. However, the potential of the NS on cell-free systems has not been sufficiently investigated yet.

In this work, we show the suitability of NS associated to URLLC and eMBB services in a RAN adopting the Cf-maMIMO scheme. Our approach relies on NS to effectively multiplex heterogeneous services in next generation RAN architectures. Several contributions in the literature have demonstrated that the massive MIMO technique is a key enabler to enhance the NS in the RAN [12], [13], [14]. Our results confirm that the Cf-maMIMO provides the desirable degree of flexibility and robustness against inter-service interference, by exploiting the sole *spatial diversity*.

We extend the theoretical framework proposed in [4] and [13], for Cf-maMIMO with conjugate beamforming, to account for the heterogeneity of QoS requirements for URLLC and eMBB services served by dedicated network slices.

Specific contributions are:

- we devise a fundamental theoretical framework envisioning the concept of NS applied to a Cf-maMIMO scenario, where we introduce the "network slicing pilot contamination" to model the inter-service interference;
- we propose a scheme for the Cf-maMIMO pilot training phase where both URLLC and eMBB users are trained **contemporarily** in the **same** coherence interval (CI), while accounting for their heterogeneous requirements;
- we evaluate the performance of the NS Cf-maMIMO in terms of spectral efficiency, achievable data rates, and outage probabilities, showing the suitability of the proposed approach.

The proposed framework enables tractable analysis of the performance and scalability of any network based on Cf-maMIMO and NS approaches to multiplex heterogeneous services with highly different QoS requirements.

The paper is organized as follows. In Section II the state of the art in Cf-maMIMO and heterogeneous services multiplexing in 5G RAN is summarized, and in Section III the proposed system model is described. Section IV illustrates the proposed multiplexing strategy for heterogeneous services, such as URLLC and eMBB, including the descriptions of the proposed approach for the training phase in UL and the customized procedures for the pilot assignment. In Sections V and VI we devise the fundamental theoretical framework for the performance evaluation of URLLC and eMBB multiplexing in a Cf-maMIMO system through NS. Finally, Section VII presents our performance evaluation results and Section VIII provides conclusions and future directions.

II. Related Work

The benefits of multi-antenna systems in a RAN exploiting multiple slices have been presented in [15]; the considered scenario involves a BS equipped with multiple antennas serving users belonging to a number of service providers via different slices. In [12], the authors demonstrate the suitability of NS on a massive MIMO communication setting in a 5G RAN to provide guaranteed performance in terms of target QoS requirements for different services. The work in [14] highlights the key role of technology enablers such as massive MIMO and NS to reduce the number of HARQ retransmissions, i.e., to address QoS latency requirements for URLLC applications.

A Cf-maMIMO scenario supporting multiple services, i.e., human and machine-to-machine communications, for heterogeneous sets of users is investigated in [13]. The analysis reveals that a conventional massive MIMO setup can significantly enhance performance and allows supporting multiple services in cellular networks without requiring additional resources. The theoretical framework proposed in [13] is extended in our work to support modern heterogeneous services with high QoS requirements such as URLLC and eMBB.

The major limiting factor to the capacity of these networks is the *pilot contamination*. Hence, PA procedures that minimise the pilot contamination have raised great interest so far [4], [16], [17], [18], [19]. The PAs for Cf-maMIMO systems range from the application of the well-known Hungarian algorithm [17], to location-based greedy PA [18], to structured PA policies that apply a fold reduction of pilot overhead if the pilot contamination is maintained at an acceptable low level [19]. It has been shown in [4] that the Cf-maMIMO with a low pilot contamination PA increases the data rate per user of 95% wrt a small cell system, while providing fairness. In this paper we show that the Cf-maMIMO asset guarantees good performance for both URLLC and eMBB services relying solely on the *spatial diversity*, independently from the applied PA assignment scheme. The Cf-maMIMO architecture enables the coexistence of heterogeneous services without any complex interference management scheme or PA assignment

procedure, e.g., a random assignment leads to performance in line with the intended KPIs.

With the application of NS to Cf-maMIMO RANs, additional sources of pilot contamination arise, due to the coexistence of multiple slices, i.e., not only among multiple users sharing the same slice. In this scenario, different slices are associated to services with specific QoS requirements, like, e.g., coexisting eMBB and URLLC, and involve subsets of the available APs serving sets of either eMBB or URLLC users. The work in [13] addresses multiple services deployed on Cf-maMIMO, but it cannot be assimilated to NS because it defines a single set of pilot sequences, without any assumption on the differentiation of the sets of resources assigned to different slices, as pointed out in [20]. We believe that, to investigate RAN slicing on a Cf-maMIMO architecture, an alternative framework for the theoretical modelling is needed to account for partitioned sets of users and possible sets of Cf-maMIMO resources assigned to different slices; and this is the main scope of this paper. The presence of different sets of pilot sequences for the two services eMBB and URLLC, introduces new challenges related to service interference, that have not been addressed yet, not even in [13].

Usually, the eMBB and URLLC traffic are multiplexed by using the superposition/puncturing scheme at the expense of the eMBB throughput's reduction. In [1], the resource allocation between eMBB and URLLC services is formulated as a bi-level optimization problem which consists of one inner problem which aims to find the optimal power and frequency resources for each URLLC and eMBB pair, and one outer problem which aims to find the optimal eMBB-URLLC pairing policy, resulting in a better eMBB loss and URLLC reliability compared to the puncturing baselines. In [8], a dynamic resource scheduling strategy is proposed for the coexistence of eMBB and URLLC traffic, based again on puncturing, by maximizing the proposed QoE-aware utility function for the whole wireless system, while guaranteeing the latency and reliability requirements of URLLC traffic. A more sophisticated approach exploits a resource allocation scheme based on an event-driven deep reinforcement learning (DRL) mechanism, which relies on a scheduler per each service, either eMBB or URLLC, to achieve long-term performance optimization [21]. Here, the eMBB and URLLC services are multiplexed on the same wireless radio frequency by using the URLLC *preemption* scheme, maximizing the average data rate of all eMBB services while satisfying the delay constraint of each URLLC service. However, the Cf-maMIMO architecture to multiplex eMBB and URLLC services is not investigated, whereas it is addressed in our paper.

The coexistence of eMBB and URLLC services is analysed also in [22] for a heterogeneous pool of users served by a single gNodeB; however, the system model is based on the classical cellular approach, not suitable for a Cf-maMIMO scenario. The cellular architecture with a serving gNodeB is also considered in [23], where the coexistence of the eMBB and URLLC services is managed by means of an AI-based framework. Our system model, instead, encompasses the Cf-maMIMO technology applied in a scenario involving 200 APs that employ dedicated resources, i.e., two distinct

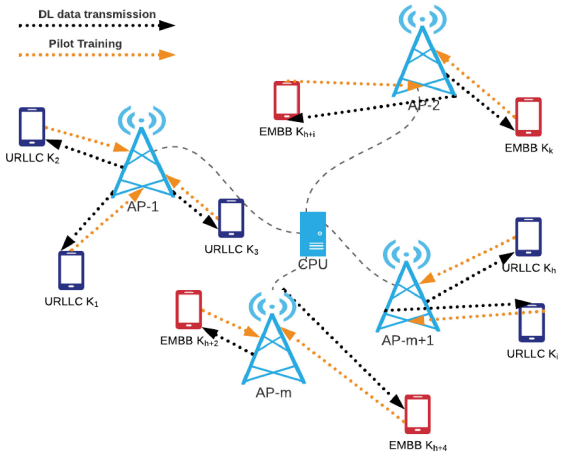

Fig. 1. Cf-maMIMO downlink scenario.

pilot sequence sets, for the two considered services. This assumption, which has never been applied before (see for example [20]), allows us to manage the coexistence, even in a cell-free environment, of service families of different nature, eMBB and URLLC, with different KPIs, i.e., the eMBB's data rate and the URLLC's latency.

We propose a general framework that represents a useful baseline to enable future performance studies for Cf-maMIMO scenarios, including those based on AI approach, which we will consider as future directions for our research.

Furthermore, we will show that the Cf-maMIMO architecture offers a unique infrastructure to exploit the spatial diversity to multiplex the eMBB and URLLC traffic through NS in the RAN. The novelty/specialty of our work wrt the related work has to be identified in the proposed system model based on the Cf-maMIMO scheme and in the assumptions introduced on the cell-free resource assignment and coherence intervals management. Those assumptions allow us to apply the concept of NS on the considered *fully distributed* radio site.

III. System Model

We consider the Cf-maMIMO downlink scenario represented in Fig. 1, with M APs, equipped with a single antenna, serving K single-antenna users. We assume a transmission scheme based on *conjugate beamforming*, which is one of the most prominent forms of linear precoding. Conjugate beamforming is based on a pre-coding matrix proportional to the conjugate of the estimated channel matrix. In the time-domain, it is also known as "time-reversal beamforming," because it is equivalent to take the convolution of each transmitted symbols' sequence with its respective conjugated and time-reversed impulse-response estimate, and sum over the K correlations. Its reverse link counterpart, at the received side, is the matched-filtering.

The users are randomly distributed in a large area. This system supports two types of services, namely eMBB and URLLC, using NS and Cf-maMIMO. We model the NS by associating the contemporary multiple data streams of URLLC and eMBB users in the RAN to one of the two partitions of the

TABLE I
SYMBOLS AND NOTATIONS

Symbol	Description
M	Total number of APs in the area
K	Total number of users in the area
M_U, M_E	Number of URLLC, eMBB APs, respectively
K_U, K_E	Number of URLLC, eMBB users, respectively
N_{sc}	Number of subcarriers
B_c	Coherence Bandwidth
T_c	Coherence time
N	Total Number of samples
N_d, N_u	Number of samples for downlink, uplink
N_p	Number of samples for training phase
$N_p^{(E)}$, $N_p^{(U)}$	Number of training samples for eMBB, URLLC respectively
y_m, $\mathbf{U}$, $\mathbf{E}$, w_m	Received signal, received training signal for URLLC, eMBB, noise term
P_E, P_U	Set of pilot sequence signals for eMBB, URLLC
ρ_u, ρ_e	URLLC, eMBB pilots power
ρ_{mk}^u, ρ_{mk}^e	Transmitted power from AP m and user k for URLLC, eMBB
$\boldsymbol{\varphi}_i^{(U)}$, $\boldsymbol{\varphi}_i^{(E)}$	i-th pilot signal for URLLC, eMBB
$\boldsymbol{\Phi}^{(U)}$, $\boldsymbol{\Phi}^{(E)}$	Sets of $N_p^{(U)}$-length and $N_p^{(E)}$-length pilot signals to be assigned to URLLC, eMBB users
$g_{mi}^{(U)}$, $g_{mi}^{(U)}$	Channel gains for the i-th pilot signal from the m-th AP for URLLC, eMBB
$\beta_{mi}^{(E)}$, $\beta_{mi}^{(U)}$	eMBB, URLLC large scale fading coefficients
$h_{mi}^{(U)}$, $h_{mi}^{(E)}$	URLLC, eMBB small scale fading coefficients
$\mathcal{CN}(\mu, \sigma)$	Gaussian distribution with mean μ and std σ
$\tilde{y}_{mi}^{(E)}$, $\tilde{y}_{mi}^{(U)}$	eMBB, URLLC received signal projection
$\hat{g}_{mj}^{(U)}$	MMSE channel estimator for URLLC
$\gamma_{mj}^{(U)}$	Mean square value of the MMSE channel estimator for URLLC
$x_{m_u \in M_U}$, $x_{m_e \in M_E}$	URLLC, eMBB transmitted signals
s_u, s_e	URLLC, eMBB transmitted symbol
r_u, r_e	URLLC, eMBB received signals
T_u, T_e	Beamforming uncertainty gain
$I_{u,u'} = 0$, $I_{e,e'} = 0$	Co-service interference
$I_{u,e}$	Inter-slice interference
n_u, n_e	Noise perceived by user u, e
SE_e^{cb}	Contention-based eMBB spectral efficiency
SE_e^{cf}	Contention-free eMBB spectral efficiency
SE_u	URLLC spectral efficiency
R_u^{DL}, R_e^{DL}	DL achievable data rate
P_u^{out}, P_e^{out}	URLLC, eMBB outage probability

pool of $K = K_U \cup K_E$ users, with $K_U = \{1, 2, \ldots, i, \ldots, h\}$ and $K_E = \{h+1, \ldots, h+i, \ldots, K\}$, which are linked to the set of APs $M = M_U \cup M_E$ partitioned in the two subsets $M_U = \{1, 2, \ldots, m_u, \ldots, |M_U|\}$ and $M_E = \{1, \ldots, m_e, \ldots, |M_E|\}$. The RAN slices associated with the two considered services are defined as:

$$eMBB_{slice} \stackrel{\text{def}}{=} (M_E, K_E) \quad (1)$$

$$URLLC_{slice} \stackrel{\text{def}}{=} (M_U, K_U) \quad (2)$$

The following derivations involve a set of symbols and notations which are summarized in Table I for the reader's convenience.

IV. URLLC AND EMBB MULTIPLEXING BY NS CF-MAMIMO

We assume a Cf-maMIMO-OFDM system as in [10]. In downlink (DL), the $N_{sc} = 2400$ subcarriers are divided into multiple resource blocks (RB), allocated to UEs such that the specific service requirements are fulfilled. According to the 5G new radio (NR) standard, we assign 12 subcarriers to a RB, such that the bandwidth of each RB is $12\Delta f$, with $\Delta f = 7.5$ kHz.

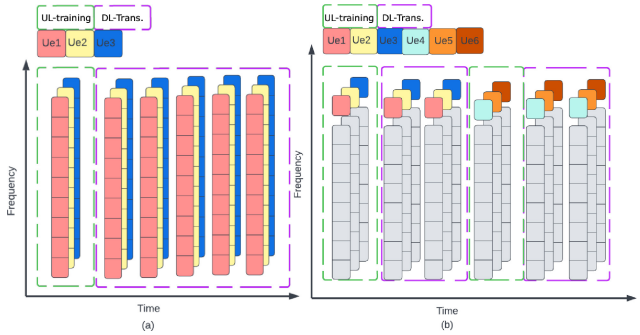

Fig. 2. Resource block allocation scheme in a coherence interval: (a) each UE occupies all RBs for eMBB; (b) each UE occupies only one RB for URLLC.

In the time domain, according to the massive MIMO operation, the subcarriers and time samples are grouped to fit the *coherence interval* (CI), which consists of a number of subcarriers and time samples where the channel response can be approximated as constant and flat-fading. If the coherence bandwidth is B_c and the coherence time is T_c, then each CI contains $N = B_c \cdot T_c$ complex-valued samples.[1]

Fig. 2 shows the RB allocation scheme in a CI, where we distinguish the CSI acquisition phase, labeled by "UL-training," and the data transmission phase, labeled by "DL-transmission." The total number of N samples is distributed among the training phase, which uses N_p samples, and the DL and UL transmissions, which use N_d and N_u samples, respectively, such that $N = N_p + N_d + N_u$ [24]. In this work, we focus only on the training phase and DL transmission, hence we have $N_u = 0$. To multiplex the eMBB and URLLC services, we adopt the resource allocation scheme shown in Fig. 2. Since the eMBB is designed to meet the demand for high-data rate transmission, each UE occupies all subcarriers, i.e., each UE is enabled to transmit with maximum bandwidth. For the URLLC case, we assume that multiple UEs can be scheduled for transmission in the same coherence interval, as the size of URLLC packets is much smaller than that of eMBB. Theoretically, assuming that each RB serves k URLLC UEs, the Cf-maMIMO-OFDM system can support a total of $kN_{sc}/12$ URLLC UEs transmitting simultaneously [10]. We formalize the RB allocation scheme described above by assuming that the URLLC utilizes a fraction δ_B of the coherence bandwidth B_c and a fraction of the downlink transmission time, as explained in Section VI. This model reflects to the calculations of the data rates for the two services, which refer to the maximum achievable performance, i.e., no queuing mechanisms are considered.

[1] A common rule of thumb is the following:
- $T_c = 1/(4 \cdot v)$ with v equal to user's velocity;
- $B_c = 1/(2T_d)$ where T_d is the delay difference between longest and shortest path.

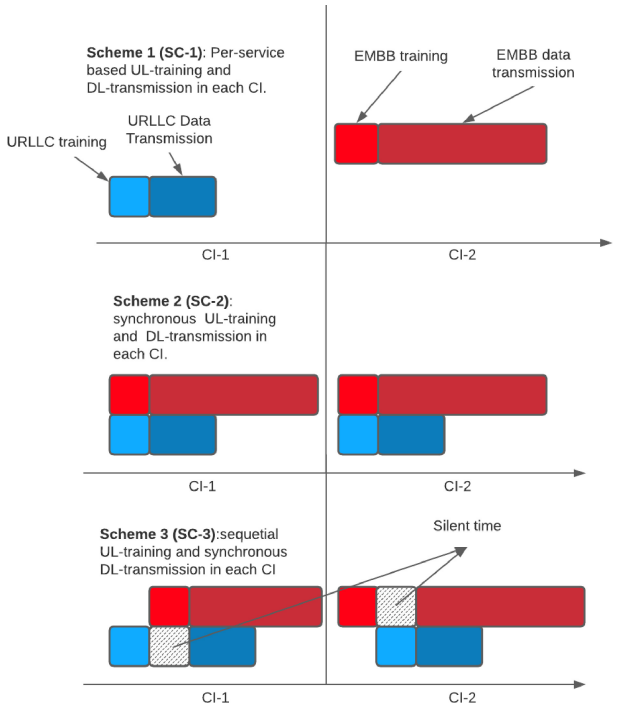

Fig. 3. Possible UL-training and DL-transmission schemes.

In the following, we analyze the training phase and propose the best suitable scheme for coexisting URLLC and eMBB services (Section IV-A); we also present two PA schemes, one simply random and the other based on a greedy selection (in Section IV-B).

A. Training Phase

The application of NS to Cf-maMIMO imposes a re-planning of the training phase. By design, the training phase is performed in *uplink*. Let's $N_p^{(E)}$ and $N_p^{(U)}$ be the number of samples assigned to the training phase of eMBB and URLLC services, respectively.

According to the strategies in [13], we distinguish the following three cases, shown in Fig. 3, differing in the applied configurations for the CIs training and transmission phases:

1) *Independent Training:* URLLC and EMBB users are *independently* trained in *different* CIs followed by its own DL transmission in the same CI. This means that the full set of N samples available in a CI are assigned either to eMBB (i.e., $N = N^{(E)}$) or to URLLC (i.e., $N = N^{(U)}$) users during the full duration of a CI. Being $N = N_p + N_d$, the samples for the training phase are $N_p^{(E)}$ and $N_p^{(U)}$ and the samples for the DL transmissions are given by either $N_d^{(E)} = N - N_p^{(E)}$ or $N_d^{(U)} = N - N_p^{(U)}$, respectively.
2) *Contemporary Training:* URLLC and eMBB users are *contemporarily* trained in the *same* CI, followed by contemporary DL transmissions in the same CI. This means that $N_p = \max\{N_p^{(E)}, N_p^{(U)}\}$ for both services. In other terms, for both services, the system uses N_p samples for the UL training phase and the remaining $N_d = N - N_p \leq N - \max\{N_p^{(E)}, N_p^{(U)}\}$ for DL transmission. Also, $N_p = \max\{N_p^{(E)}, N_p^{(U)}\}$ guarantees orthogonality between users but it is not sufficient to prevent the interference between services.
3) *Sequential Training:* URLLC and eMBB users are *sequentially* trained in the *same* CI, followed by contemporary DL transmissions in the same CI. Hence, we have $N_p = N_p^{(E)} + N_p^{(U)} \leq 2 \cdot \max\{N_p^{(E)}, N_p^{(U)}\}$, with the constraint that one type of users is silent while the other performs the training phase. Therefore, the DL uses a number of samples $N_d = N - N_p \leq N - 2 \cdot \max\{N_p^{(E)}, N_p^{(U)}\}$.

To define *independent* pilot sequences using $N_p^{(U)}$ and $N_p^{(E)}$ training samples for URLLC and eMBB users, respectively, we assume that

$$N_p^{(U)} = |K_U| \tag{3}$$
$$N_p^{(E)} = |K_E|. \tag{4}$$

The conditions (3) and (4) imply that user-coherent interference doesn't exist. However, the orthogonality is not ensured between P_U and P_E, giving rise to *inter-service interference*.

Depending on the applied training phase configuration, under the assumption of per service pairwise orthogonality of the sequence pilot sets, we have:

1) For *independent training*, URLLC and eMBB users will not experience any kind of inter-users or inter-service interference. Hence, based on the type of users active in the current CI, the signal received by the m-th AP during the training phase will by either: $\mathbf{y}_m = \mathbf{U} + \mathbf{w}_m$ or $\mathbf{y}_m = \mathbf{E} + \mathbf{w}_m$ for all N_p samples in the CI for each of the two services, where the three contributions are related respectively to the training of the K_U URLLC users, i.e., $\mathbf{U} \in \mathbb{C}^{N_p^{(U)} \times 1}$, and the K_E eMBB users, i.e., $\mathbf{E} \in \mathbb{C}^{N_p^{(E)} \times 1}$, and, finally, to the noise term $\mathbf{w}_m \in \mathbb{C}^{\max\{N_p^{(E)}, N_p^{(U)}\} \times 1}$. The elements of the three terms are all i.i.d random variables distributed according to a complex normal distribution, i.e., $\sim \mathcal{CN}(0, 1)$. It is important to observe that the sum of the complex vectors $\mathbf{U}$, $\mathbf{E}$, $\mathbf{w}_m$ is defined for equal-size vector spaces.
2) For *contemporary training*, URLLC and eMBB users will experience only *inter-service interference* and the signal received by the m-th AP is

$$\mathbf{y}_m = \mathbf{U} + \mathbf{E} + \mathbf{w}_m \tag{5}$$

for $N_p = \max\{N_p^{(E)}, N_p^{(U)}\}$ samples in the CI.
3) For *sequential training*, URLLC and eMBB users will not experience any kind of user or inter-service interference, as in the first case, and similarly the signal received by m-th AP results either $\mathbf{y}_m = \mathbf{U} + \mathbf{w}_m$ or $\mathbf{y}_m = \mathbf{E} + \mathbf{w}_m$, respectively for the $N_p^{(U)}$ and $N_p^{(E)}$ samples in the CI.

Despite the independent and sequential trainings don't provide any interference among both users and services, they

present significant drawbacks. In the case of independent training, as shown in Fig. 3, each available CI is assigned to the sole transmission of either URLLC or eMBB, with subsequent under-utilization of the available resources (more evident in the case of URLLC transmissions, based on a very short payload), and increase of URLLC latency. Hence, this scheme is not suitable to fulfil URLLC latency requirements.

The sequential training, instead, violates both URLLC reliability and latency requirements, being the training done in the absence of interference, whereas the transmissions are simultaneous to eMBB traffic, but rely on a pilot assignment based on non-accurate channel estimations, thus impacting the reliability of URLLC transmissions. Moreover, the sequential training adds a delay to the URLLC latency.

Therefore, for the optimal coexistence of URLLC and eMBB services, due to their specific QoS requirements, the only possible scheme is the contemporary training of URLLC and eMBB users in the same CI. This is the scheme adopted throughout the subsequent analyses presented in this paper.

Based on the type of service, i.e., URLLC and eMBB, we define two sets of pilot sequence signals P_E and P_U as:

$$P_U = \left\{ \sqrt{N_p^{(U)}\rho_u}\boldsymbol{\varphi}_i^{(U)} \in \mathbb{C}^{N_p^{(U)}\times 1} | i \in K_U \right\} \tag{6}$$

$$P_E = \left\{ \sqrt{N_p^{(E)}\rho_e}\boldsymbol{\varphi}_j^{(E)} \in \mathbb{C}^{N_p^{(E)}\times 1} | j \in K_E \right\} \tag{7}$$

where

$$\left\{ \sqrt{N_p^{(U)}\rho_u}\boldsymbol{\Phi}^{(U)} \right\} \in \mathbb{C}^{N_p^{(U)}\times |K_U|}$$
$$\left\{ \sqrt{N_p^{(E)}\rho_e}\boldsymbol{\Phi}^{(E)} \right\} \in \mathbb{C}^{N_p^{(E)}\times |K_E|}$$

are the sets of $N_p^{(U)}$-length and $N_p^{(E)}$-length pilot signals to be assigned to URLLC and eMBB users, with ρ_u and ρ_e the UL pilot powers, and $\boldsymbol{\Phi}^{(U)} = [\boldsymbol{\varphi}_1^{(U)} \dots \boldsymbol{\varphi}_i^{(U)} \dots \boldsymbol{\varphi}_{K_U}^{(U)}]$ and $\boldsymbol{\Phi}^{(E)} = [\boldsymbol{\varphi}_1^{(E)} \dots \boldsymbol{\varphi}_j^{(E)} \dots \boldsymbol{\varphi}_{K_E}^{(E)}]$. Hence, for the contemporary scheme, the general expression for the signal received by the m-th AP during the training phase of the massive MIMO conjugate beamforming scheme, when all K users transmit the pilots simultaneously, is given by (5) with

$$\mathbf{U} = \sqrt{N_p^{(U)}\rho_{\mathrm{u}}} \sum_{i\in K_U} g_{mi}^{(U)}\boldsymbol{\varphi}_i^{(U)}$$
$$\mathbf{E} = \sqrt{N_p^{(E)}\rho_{\mathrm{e}}} \sum_{i\in K_E} g_{mi}^{(E)}\boldsymbol{\varphi}_i^{(E)} \tag{8}$$

The channel gains $g_{mi}^{(U)}$ and $g_{mi}^{(E)}$ are defined as [4]:

$$g_{mi}^{(U)} = \sqrt{\beta_{mi}^{(U)}}h_{mi}^{(U)} \quad \text{for all} \quad i \in K_U$$
$$g_{mi}^{(E)} = \sqrt{\beta_{mi}^{(E)}}h_{mi}^{(E)} \quad \text{for all} \quad i \in K_E, \tag{9}$$

with the large scale fading coefficients $\beta_{mi}^{(E)}$ and $\beta_{mi}^{(U)}$, and the small scale fading coefficients $h_{mi}^{(U)} \sim \mathcal{CN}(0,1)$ and $h_{mi}^{(E)} \sim \mathcal{CN}(0,1)$, modeled as i.i.d. complex Gaussian RVs according to [25, Sec. 2.5.2]. The assumption of independent small-scale fading is fully justified in the proposed scenario, because APs and users are distributed over a wide area, such that the set of scatterers is likely to be different for each pair AP-user.

Given the two sets of pilot sequence signals P_U and P_E in (6) and (7), for each of the two sets of users K_U and K_E, we derive the following projections. For user $i \in K_E$ we have:

$$\tilde{y}_{mi}^{(E)} \triangleq \boldsymbol{\varphi}_i^{(E)H}\mathbf{y}_m = \boldsymbol{\varphi}_i^{(E)H}[\mathbf{U} + \mathbf{E} + \mathbf{w}_m] \tag{10}$$

where $\mathbf{U}$ and $\mathbf{E}$ are given by (8). Taking into account the assumption of the pair-wise orthogonality, i.e.:

$$\boldsymbol{\varphi}_i^{(U)H}\boldsymbol{\varphi}_t^{(U)} = \begin{cases} ||\left(\boldsymbol{\varphi}_t^{(U)}\right)||^2 = \boldsymbol{I}_t & \text{if } t = i \in K_U \\ 0 & \text{otherwise} \end{cases}$$

we get:

$$\tilde{y}_{mi}^{(E)} = \sqrt{N_p^{(E)}\rho_{\mathrm{e}}}g_{mi}^{(E)} + \sqrt{N_p^{(U)}\rho_{\mathrm{u}}} \sum_{s\in K_U} g_{ms}^{(U)}\boldsymbol{\varphi}_i^{(E)H}\boldsymbol{\varphi}_s^{(U)} + \boldsymbol{\varphi}_i^{(E)H}\mathbf{w}_m \tag{11}$$

Similarly, for user $j \in K_U$ the projection is given by:

$$\tilde{y}_{mj}^{(U)} \triangleq \boldsymbol{\varphi}_j^{(U)H}\mathbf{y}_m = \sqrt{N_p^{(U)}\rho_{\mathrm{u}}}g_{mj}^{(U)} + + \sqrt{N_p^{(E)}\rho_{\mathrm{e}}} \sum_{t\in K_E} g_{mt}^{(E)}\boldsymbol{\varphi}_j^{(U)H}\boldsymbol{\varphi}_t^{(E)} + \boldsymbol{\varphi}_j^{(U)H}\mathbf{w}_m \tag{12}$$

given the pair-wise orthogonality condition in the eMBB case:

$$\boldsymbol{\varphi}_i^{(E)H}\boldsymbol{\varphi}_s^{(E)} = \begin{cases} ||\left(\boldsymbol{\varphi}_s^{(E)}\right)||^2 = \boldsymbol{I}_s & \text{if } s = i \in K_E \\ 0 & \text{otherwise} \end{cases}$$

The second term in both (11) and (12) represents the *network slicing pilot contamination*.

Based on the received projection $\tilde{y}_{mj}^{(U)}$ or $\tilde{y}_{mi}^{(E)}$, the CPU evaluates the MMSE estimates $\hat{g}_{mj}^{(U)}$ and $\hat{g}_{mi}^{(E)}$ needed to apply the precoding for the conjugate beamforming. By assumption, the large scale fading coefficients $\hat{g}_{mj}^{(U)}$ are known to be complex-Gaussian distributed, i.e., $\sim \mathcal{CN}(0, \beta_j^{(U)})$, hence the MMSE estimator for the URLLC case is

$$\hat{g}_{mj}^{(U)} = \frac{\mathbb{E}\left\{g_{mj}^{(U)}\tilde{y}_{mj}^{(U)}\right\}}{\mathbb{E}\left\{|\tilde{y}_{mj}^{(U)}|^2\right\}}\tilde{y}_{mj}^{(U)} = c_{mj}^{(U)}\tilde{y}_{mj}^{(U)} \tag{13}$$

where

$$c_{mj}^{(U)} = \frac{\sqrt{N_p^{(U)}\rho_u}\beta_{mj}^{(U)}}{1 + \sqrt{N_p^{(E)}\rho_{\mathrm{e}}}\sum_{t\in K_E}\beta_{mt}^{(E)}|\boldsymbol{\varphi}_j^{(U)H}\boldsymbol{\varphi}_t^{(E)}|^2} \tag{14}$$

and, as in [26], its mean square value $\gamma_{mi}^{(U)}$ is defined as:

$$\gamma_{mj}^{(U)} = \mathbb{E}\left\{|\hat{g}_{mj}^{(U)}|^2\right\} = \sqrt{N_p^{(U)}\rho_u}\beta_{mj}^{(U)}c_{mj}^{(U)} = = \frac{N_p^{(U)}\rho_u\left(\beta_{mj}^{(U)}\right)^2}{1 + \sqrt{N_p^{(E)}\rho_{\mathrm{e}}}\sum_{t\in K_E}\beta_{mt}^{(E)}|\boldsymbol{\varphi}_j^{(U)H}\boldsymbol{\varphi}_t^{(E)}|^2} \tag{15}$$

Being the channels of the single-antennas APs statistically identical, $\gamma_{mj}^{(U)}$ is the same for all M_U APs [26].

Algorithm 1 Random PA

Require: $\mathbf{\Phi^{(U)}}$, $\mathbf{\Phi^{(E)}}$, K_U, K_E
Ensure: $A_u = [\boldsymbol{\varphi}_1^{(U)} \dots \boldsymbol{\varphi}_i^{(U)} \dots \boldsymbol{\varphi}_{K_U}^{(U)}]$ and $A_e = [\boldsymbol{\varphi}_1^{(E)} \dots \boldsymbol{\varphi}_i^{(E)} \dots \boldsymbol{\varphi}_{K_E}^{(E)}]$
while $i \in K_U$ **do**
  $A_u[i]$ =Random selection of $\boldsymbol{\varphi}_i^{(U)} \in \mathbf{\Phi^{(U)}}$
end while
while $i \in K_E$ **do**
  $A_e[i]$ =Random selection of $\boldsymbol{\varphi}_i^{(E)} \in \mathbf{\Phi^{(E)}}$
end while

Algorithm 2 Greedy PA

Require: $\mathbf{\Phi^{(U)}}$, $\mathbf{\Phi^{(E)}}$, K_U, K_E
Ensure: $A_u = [\boldsymbol{\varphi}_1^{(U)} \dots \boldsymbol{\varphi}_j^{(U)} \dots \boldsymbol{\varphi}_{K_U}^{(U)}]$ and $A_e = [\boldsymbol{\varphi}_1^{(E)} \dots \boldsymbol{\varphi}_j^{(E)} \dots \boldsymbol{\varphi}_{K_E}^{(E)}]$
while $j \in K_U$ **do**
  $A_u[j] =$ select $\boldsymbol{\varphi}_j^{(U)} = \arg\min_{\boldsymbol{\varphi}_j^{(U)}} \sum_{m \in M_U} \Xi_E$
  s.t $\boldsymbol{\varphi}_j^{(U)} \in \mathbf{\Phi^{(U)}}$
end while
while $i \in K_E$ **do**
  $A_e[i] =$ select $\boldsymbol{\varphi}_i^{(E)} = \arg\min_{\boldsymbol{\varphi}_{i(E)}} \sum_{m \in M_E} \Xi_U$
  s.t $\boldsymbol{\varphi}_i^{(E)} \in \mathbf{\Phi^{(E)}}$
end while

The channel estimation error is defined as $\epsilon_j^{(U)} = \hat{g}_j^{(U)} - g_j^{(U)}$ where $\epsilon_j^{(U)} \sim \mathcal{CN}(0, \beta_j^{(U)} - \gamma_j^{(U)})$ is independent from $\hat{g}_j^{(U)} \sim \mathcal{CN}(0, \gamma_j^{(U)})$. The mean square error has a variance of $\mathbb{E}\{|\epsilon_j^{(U)}|^2\} = \beta_i^{(U)} - \gamma_j^{(U)}$ [27]. Similar derivations can be done to obtain the channel estimate $\hat{g}_{mi}^{(E)}$ for $i \in K_E$.

B. Pilot Assignment Procedures

We consider two PAs, customized for the specific scenario of Cf-maMIMO URLLC and eMBB sliced services. The *Random PA*, described in Algorithm 1, is a very simple assignment method constrained only by the user's type. With this strategy the user will randomly receive a pilot out from the pilots' set. Users of different services that are in close vicinity could experience inter-service interference which is not taken into account for the selection of the assigned pilots. For the sake of Algorithm 1's readability, we introduce the index i to address the users in both sets K_U, K_E and the positioning within the output arrays A_u, A_e.

The *Greedy PA*, described in Algorithm 2, instead, accounts for the inter-service interference, i.e., for the *network slice pilot contamination*. The pilot contamination is expressed for the two services by the terms $\sum_{t \in K_E} g_{mt}^{(E)} \boldsymbol{\varphi}_j^{(U)H} \boldsymbol{\varphi}_t^{(E)}$ and $\sum_{s \in K_U} g_{ms}^{(U)} \boldsymbol{\varphi}_i^{(E)H} \boldsymbol{\varphi}_s^{(U)}$ in (11) and (12). Their variances are given by:

$$\mathbb{E}\left\{ \left| \sum_{t \in K_E} g_{mt}^{(E)} \boldsymbol{\varphi}_j^{(U)H} \boldsymbol{\varphi}_t^{(E)} \right|^2 \right\} = \sum_{t \in K_E} \beta_{mt}^{(E)} |\boldsymbol{\varphi}_j^{(U)H} \boldsymbol{\varphi}_t^{(E)}|^2$$

$$\mathbb{E}\left\{ \left| \sum_{s \in K_U} g_{ms}^{(U)} \boldsymbol{\varphi}_i^{(E)H} \boldsymbol{\varphi}_s^{(U)} \right|^2 \right\} = \sum_{s \in K_U} \beta_{ms}^{(U)} |\boldsymbol{\varphi}_i^{(E)H} \boldsymbol{\varphi}_s^{(U)}|^2$$

Each user will be assigned the pilot sequence which minimizes the network slice pilot contamination summed over all the APs, according to the type of service. For the user $j \in K_U$ the assigned pilot is found by solving (P1), for the user $i \in K_E$ by solving (P2):

$$\arg\min_{\boldsymbol{\varphi}_j^{(U)}} \sum_{m \in M_U} \sum_{\substack{t \in K_E, \\ \boldsymbol{\varphi}_j^{(U)} = \boldsymbol{\varphi}_t^{(E)}}} \beta_{mt}^{(E)} |\boldsymbol{\varphi}_j^{(U)H} \boldsymbol{\varphi}_t^{(E)}|^2 \quad \text{(P1)}$$

$$\arg\min_{\boldsymbol{\varphi}_i^{(E)}} \sum_{m \in M_E} \sum_{\substack{s \in K_U, \\ \boldsymbol{\varphi}_i^{(E)} = \boldsymbol{\varphi}_s^{(U)}}} \beta_{ms}^{(U)} |\boldsymbol{\varphi}_i^{(E)H} \boldsymbol{\varphi}_s^{(U)}|^2 \quad \text{(P2)}$$

For the sake of readability, we define the following simplified notations for the problems P1 and P2 in Algorithm 2, where indexes i and j are in accordance with previous formulas:

$$\Xi_E = \sum_{\substack{t \in K_E, \\ \boldsymbol{\varphi}_j^{(U)} = \boldsymbol{\varphi}_t^{(E)}}} \beta_{mt}^{(E)} |\boldsymbol{\varphi}_j^{(U)H} \boldsymbol{\varphi}_t^{(E)}|^2$$

$$\Xi_U = \sum_{\substack{s \in K_U, \\ \boldsymbol{\varphi}_i^{(E)} = \boldsymbol{\varphi}_s^{(U)}}} \beta_{ms}^{(U)} |\boldsymbol{\varphi}_i^{(E)H} \boldsymbol{\varphi}_s^{(U)}|^2.$$

V. Downlink Transmission

Let s_u, with $u \in K_U$ and $\mathbb{E}\{|s_u|^2\} = 1$, be the symbol to be transmitted to URLLC users, and s_e, with $e \in K_E$ and $\mathbb{E}\{|s_e|^2\} = 1$, the symbol to be transmitted to eMBB users. We assume that the symbols are uncorrelated, i.e., $\mathbb{E}\{|s_e s_u|^2\} = 0$. Based on the assumption of channel reciprocity, the signals transmitted by the APs $m_u \in M_U$ and $m_e \in M_E$ that apply the conjugate beamforming precoding based on the MMSE channel estimation, can be written as:

$$x_{m_u \in M_U} = \sum_{u \in K_U} \sqrt{N_d^{(U)} \rho_{\mathrm{u}}} \hat{g}_{m_u, u} s_u \quad (16)$$

$$x_{m_e \in M_E} = \sum_{e \in K_E} \sqrt{N_d^{(E)} \rho_{\mathrm{e}}} \hat{g}_{m_e, e} s_e \quad (17)$$

with the conditions $\mathbb{E}\{|x_{m_u}|^2\} \leq \rho_{\mathrm{u}}$, $\mathbb{E}\{|x_{m_e}|^2\} \leq \rho_{\mathrm{e}}$. In this Cf-maMIMO scenario, the generic i-th user receives a signal resulting from the superposition of (16) and (17). In particular, the signals received by the URLLC user $u \in K_U$ and the eMBB user $e \in K_E$ are expressed as (in the following we omit the superscripts $^{(U)}$ and $^{(E)}$ to improve the clarity of the expressions - the terms are distinguished by the subscripts):

$$\begin{aligned} r_u &= \sum_{m_u \in M_U} g_{m_u, u} x_{m_u} + \sum_{m_e \in M_E} g_{m_e, u} x_{m_e} + n_u = \\ &= \sum_{m_u \in M_U} \sum_{u' \in K_U} \sqrt{N_d^{(U)} \rho_{\mathrm{u}}} g_{m_u, u} \hat{g}_{m_u, u'} s_{u'} + \\ &\quad + \sum_{m_e \in M_E} \sum_{e \in K_E} \sqrt{N_d^{(E)} \rho_{\mathrm{e}}} g_{m_e, u} \hat{g}_{m_e, e} s_e + n_u \end{aligned} \quad (18)$$

and

$$r_e = \sum_{m_e \in M_E} g_{m_e,e} x_{m_e} + \sum_{m_u \in M_U} g_{m_u,e} x_{m_u} + n_e$$
$$= \sum_{m_e \in M_E} \sum_{e' \in K_E} \sqrt{N_d^{(E)} \rho_{\mathrm{e}}} g_{m_e,e} \hat{g}_{m_e,e'} s_{e'} +$$
$$+ \sum_{m_u \in M_U} \sum_{u \in K_U} \sqrt{N_d^{(E)} \rho_{\mathrm{e}}} g_{m_u,e} \hat{g}_{m_u,u} s_u + n_e \quad (19)$$

that can be expressed in a compact form [28] as:

$$r_u = S_u s_u + T_u s_u + I_{u,u'} s_{u'} + I_{u,e} s_e + n_u \quad (20)$$

where n_u is the effective noise perceived by the user *u*, and

$$S_u = \mathbb{E}\left\{ \sum_{m_u \in M_U} \sqrt{N_d^{(U)} \rho_{\mathrm{u}}} g_{m_u,u} \hat{g}_{m_u,u} \right\}$$
$$T_u = \sum_{m_u \in M_U} \sqrt{N_d^{(U)} \rho_{\mathrm{u}}} g_{m_u,u} \hat{g}_{m_u,u} - \mathbb{E}\left\{ \sum_{m_u \in M_U} \sqrt{N_d^{(U)} \rho_{\mathrm{u}}} g_{m_u,u} \hat{g}_{m_u,u} \right\}$$
$$I_{u,u'} = \sum_{\substack{u' \in K_U \\ u' \neq u}} \sum_{m_u \in M_U} \sqrt{N_d^{(U)} \rho_{\mathrm{u}}} g_{m_u,u'} \hat{g}_{m_u,u'}$$
$$I_{u,e} = \sum_{e \in K_E} \sum_{m_e \in M_E} \sqrt{N_d^{(E)} \rho_{\mathrm{e}}} g_{m_e,u} \hat{g}_{m_e,e}$$

are, respectively, a deterministic factor S_u scaling the desired signal of the URLLC user $u \in K_U$ as given by the conjugate beamforming precoding; the contribution T_u in the received signal related to the *beamforming uncertainty gain*; the interference $I_{u,u'}$ with the signals by other URLLC users $u' \in K_U \setminus \{u\}$, which is $I_{u,u'} = 0$ under our assumption of orthogonality between users of the same service; the *inter-slice interference* $I_{u,e}$ between URLLC user *u* and all eMBB users.

VI. Performance Metrics

We define three metrics to measure the performance of the proposed Cf-maMIMO system with NS applied to URLLC and eMBB served users: the spectral efficiency, the achievable average data rate and the outage probability.

The DL spectral efficiency for users $u \in K_U$, under the condition $M >> K$, is defined as [28]:

$$SE_u = \log_2\left(1 + \frac{|S_u|^2}{\mathbb{E}\{|I_{u,u'}|^2\} + \mathbb{E}\{|I_{u,e}|^2\} + 1}\right) =$$
$$= \log_2\left(1 + \frac{|S_u|^2}{\mathbb{E}\{|I_{u,e}|^2\} + 1}\right) \quad (21)$$

where, as derived in the Appendix:

$$|S_u|^2 = N_d^{(U)} \rho_{\mathrm{u}} \left(\sum_{m_u \in M_U} \gamma_{m_u,u} \right)^2 \quad (22)$$

and

$$\mathbb{E}\left\{|I_{u,e}|^2\right\} = N_d^{(E)} \rho_{\mathrm{e}} \sum_{e \in K_E} \sum_{m_e \in M_E} \gamma_{m_e,e} \beta_{m_e,u}. \quad (23)$$

The expression (21) holds under the condition $M >> K$: as demonstrated in [26], for large values of M the contribution of the beamforming uncertainty gain in the received signal is negligible.

For the user $e \in K_E$ we define the corresponding terms S_e, $I_{e,e'}$ and $I_{e,u}$ and derive the expression for the spectral efficiency. However, in light of the adopted RB allocation strategy, since the eMBB payload has a bigger size than the URLLC, we assume that URLLC DL transmissions are "puncturing" the DL time slot, resulting in the utilization of a portion of the total DL time T_d.

The DL time slot is given by $T_d = T_c(1 - N_p/N)$, with $N = B_c T_c$. We identify two portions in T_d: the *contention-based DL transmission time* defined as $T_{cb} = w_{cb} T_d$, where simultaneous URLLC and eMBB transmissions cause inter-service interference; and the *contention-free DL transmission time* $T_{cf} = T_d - T_{cb}$, where only eMBB users transmit and will not experience any kind of inter-user or inter-slice interference. The weighting factor $w_{cb} \in (0, \frac{1}{2})$ represents the estimated time fraction of simultaneous DL transmissions.

Hence, the total spectral efficiency for eMBB users is:

$$SE_e = SE_e^{cb} + SE_e^{cf} \quad (24)$$

where

$$SE_e^{cb} = \log_2\left(1 + \frac{|S_e|^2}{\mathbb{E}\{|I_{e,e'}|^2\} + \mathbb{E}\{|I_{e,u}|^2\} + 1}\right)$$
$$= \log_2\left(1 + \frac{|S_e|^2}{\mathbb{E}\{|I_{e,u}|^2\} + 1}\right)$$
$$SE_e^{cf} = \log_2\left(1 + \frac{|S_e|^2}{\mathbb{E}\{|I_{e,e'}|^2\} + \mathbb{E}\{|I_{e,u}|^2\} + 1}\right)$$
$$= \log_2\left(1 + |S_e|^2\right)$$

are, respectively, the *contention-based eMBB spectral efficiency term* SE_e^{cb} related to T_{cb} and the *contention-free eMBB spectral efficiency term* related to T_{cf}.

Therefore, we define the achievable data rates R_u^{DL} and R_e^{DL} for DL transmissions of the users $u \in K_u$ and $e \in K_e$, respectively, as functions of the spectral efficiency SE_u and SE_e, the coherence bandwidth B_c, the *contention-based DL transmission time* T_{cb} and the *contention-free DL transmission time* T_{cf} as:

$$R_u^{DL} = \delta_B \cdot B_c \cdot T_{cb} \cdot SE_u \quad (25)$$
$$R_e^{DL} = B_c \cdot \left\{ T_{cb} \cdot SE_e^{cb} + T_{cf} \cdot SE_e^{cf} \right\} \quad (26)$$

where δ_B is the fraction of the coherence bandwidth assigned to URLLC users according to our RB assignment scheme.

Finally, we define the outage probability as a metric to evaluate the *scalability* of Cf-maMIMO supporting NS. The eMBB and URLLC services have specific payload size requirements

TABLE II
SIMULATION PARAMETERS

Parameter [Unit]	Value
Simulation Area [km^2]	1
Access points in the area, M	200
$\lvert M_E\rvert = \lvert M_U\rvert$ access points per service	100
$\rho_u^{(UL)}\lvert_{max} = \rho_e^{(UL)}\lvert_{max}$ [mW]	100
$\rho_u^{(DL)}\lvert_{max} = \rho_e^{(DL)}\lvert_{max}$ [mW]	200
Coherence interval length, N	$5 \cdot 10^4$
Shadowing F_{km}	$\mathcal{N}(0, 4^2)$
Coherence bandwidth B_c [MHz]	1
eMBB payload size b_e [Bytes]	1500
URLLC payload size b_u [Bytes]	32

b_u and b_e, respectively. The outage probability refers to a network's operating condition that doesn't support the transmission of packets of these fixed sizes of b_u and b_e bits. Then, if $R_u^{th} = f(b_u)$ and $R_e^{th} = f(b_e)$ are the data rate threshold values for the URLLC and eMBB services, the outage probability for the specific user is defined as

$$P_u^{out} = \Pr\left[R_u^{DL} < R_u^{th}\right] \text{ for } u \in K_U \tag{27}$$

$$P_e^{out} = \Pr\left[R_e^{DL} < R_e^{th}\right] \text{ for } e \in K_E \tag{28}$$

VII. PERFORMANCE EVALUATION

We investigate the performance of the proposed network sliced Cf-maMIMO system for different sizes of the pool of users, that is $20 \leq K \leq 200$, still fulfilling the design condition of Cf-maMIMO, $M >> K$, being $M = 200$ the total number of APs in the area with $M = M_E + M_U$ and $|M_E| = |M_U|$.

A. Simulation Setup

We consider a square area of 1 km^2 with M APs and K users, with $M_U = M/2$ APs and $K_U = K/2$ users (UEs) assigned to URLLC and $M_E = M/2$ APs and $K_E = K/2$ UEs assigned to eMBB. To avoid boundary effects and to imitate a network spread over an infinite area, the square is wrapped around. Regardless of service, during the UL training phase we assume a maximum transmission power of $\rho_u^{(UL)}|_{max} = \rho_e^{(UL)}|_{max} = 100$ mW for each user. For the DL transmission, the available maximum total power is $\rho_u^{(DL)}|_{max} = \rho_e^{(DL)}|_{max} = 200$ mW. All values of simulation parameters are listed in Table II.

The APs apply a centralized power allocation scheme and assign to each users an amount of power given by

$$\rho_{mk}^u = \rho_u^{tot} \frac{\left(\beta_{km}^u\right)^v}{\sum_{(k,m)}\left(\beta_{km}^u\right)^v}$$

with $k \in K_U$, $m \in M_U$ and $v \in [0, 1]$. The value of $v = 0$ implies that the assigned power is a fraction of the total available power. The value of $v = 1$ implies that the assigned power relies on the channel condition between the AP m and the considered user k. Similarly, for the eMBB APs and users. According to [25], we assume that the length of a CI is $200 \leq N \leq O(10^4)$, where $N = 200$ corresponds to a network with high mobility and high channel dispersion,

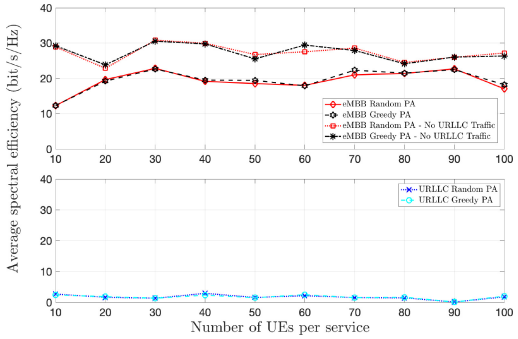

Fig. 4. Spectral efficiency of the two services URLLC (lower plot) and eMBB (upper plot) multiplexed in the same area in the Cf-maMIMO system for the two considered PAs. For the eMBB, the spectral efficiency is shown for both scenarios with and without URLLC traffic.

whereas $N = O(10^4)$ reflects a network with low user mobility and low channel dispersion. We set $N = 5 \cdot 10^4$. The APs are deployed in a urban dense micro-cell scenario matching the 3GPP model for the 2 GHz band [29]. According to that model, for each m-AP and k-UE, we evaluate the channel gains as:

$$\beta_{km}[dB] = -30.5 - 36.7 \log_{10}(d_{km}/d_0) + F_{km} \tag{29}$$

where the d_{km} is the 3D distance from the m-th AP to the k-th UE, $d_0 = 1$ m is the reference distance, and $F_{km} \sim \mathcal{N}(0, 4^2)$ is the shadowing term. The shadowing fading from the pair AP m and UE k to the pair AP j and UE i has a correlation given by:

$$\mathbb{E}\left[F_{km}F_{ij}\right] = \begin{cases} 4^2 2^{\Delta_{ki}/9\ m} & \text{if } m = j \\ 0 & \text{if } m \neq j \end{cases} \tag{30}$$

where Δ_{ki} is the distance of user k from user i. The second row reflects the shadowing effects for different APs that is assumed to be zero. The reason is that APs are typically distributed in the network at a distance larger than tens of meters and purposely deployed to view the deployment area from different directions than other APs. The coherence bandwidth is assumed to be $B_c = 1$ MHz. Finally, the eMBB packet payload size is set to $b_e = 1500$ bytes and the URLLC size to $b_u = 32$ bytes, according to the standard.

B. Results and Discussion

We show the average spectral efficiencies and the cumulative distribution functions (CDFs) of the throughput of URLLC and eMBB users for the two different PA schemes against the number of users. To show the benefits of the spatial diversity offered by the Cf-maMIMO, we analyze also the case of eMBB traffic only, without any interference from URLLC users. The average spectral efficiency vs. the number of UEs per service is depicted in Fig. 4 for the eMBB with and without URLLC traffic (upper plot) and for the URLLC (lower plot). As expected, in a single-service deployment scenario, the spectral efficiency is higher with respect to the multi-service scenario and this reflects in a higher throughput of the eMBB users in the absence of URLLC traffic, as shown in Fig. 5 for the two exemplary cases of 40 and 100 UEs. Apparently, the

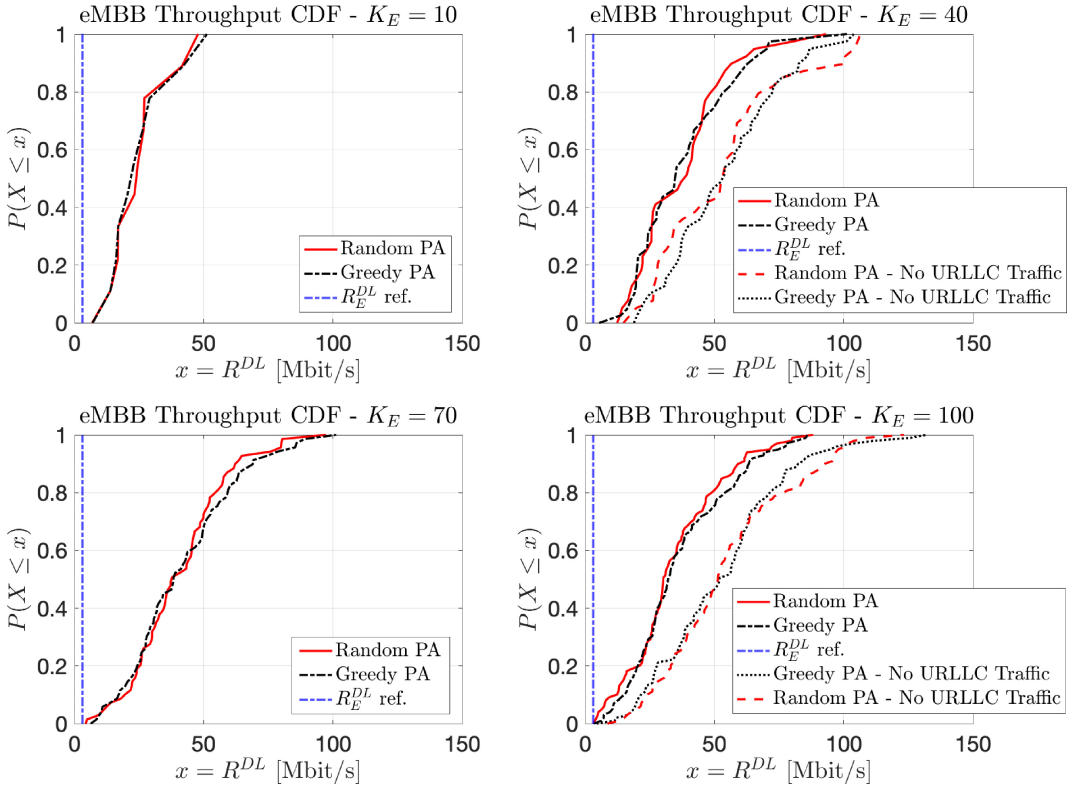

Fig. 5. CDFs of the eMBB throughput for different numbers of UEs for the two considered PAs.

PA scheme does not have any impact on the performance, but this point deserves further investigations.

Figures 5 and 6 show the CDFs of the throughput for eMBB and URLLC services, respectively, for the two considered PA schemes in the proposed Cf-maMIMO RAN. We notice that the throughput does not show any improvement when the more sophisticated greedy PA scheme is applied. The random and greedy PA curves are very close, which confirms the effectiveness of our approach based on Cf-maMIMO that exploits the spatial diversity. In this scenario, which involves a number of APs much greater than the number of UEs, as design condition for Cf-maMIMO systems, the less demanding random approach can be applied, because the spatial diversity guarantees that the reference requirements shown by the straight dash-dotted lines in the figures, are fulfilled for both services even with the random PA. As a future work, we will explore the use of more sensible pilots allocation schemes and will infer whether such schemes can allow us to relax the Cf-maMIMO condition $M >> K$ and get the number of APs closer or even below to the number of UEs.

Increasing the number of users from 10 to 100 per service, while keeping constant the number of APs, $M = 200$, produces at first an improvement of the throughput (from 10 to 40 UEs), but then a slight performance downgrade in the case of multiplexed eMBB and URLLC. This is related to the main condition of the Cf-maMIMO asset, that is $M >> K$, i.e., the number of APs must be much greater than the number of served users. Indeed this effect is not evident in the eMBB CDFs without URLLC traffic, because in this case the number of APs is twice the number of UEs. When M approaches the number of UEs in the area, the spectral efficiency expression (21) should account also for the beamforming uncertainty gain. For the URLLC, we observe a similar behavior, with the throughput re-scaled according to the URLLC traffic characteristics. Moreover, Fig. 6 shows that for low levels of interference, i.e., for small numbers of users (i.e., 10 or 40), the greedy PA scheme slightly outperforms the random PA; instead, at high interference regimes, i.e., with 70 or 100 users per service, the adopted PA scheme does not have any effect. Finally, looking at the intersection between the throughput CDFs curves and the reference values per service R_u^{th} and R_e^{th} reported in Figures 5 and 6, we may infer that the service slicing in the proposed Cf-maMIMO RAN guarantees the fulfillment of the QoS requirements for eMBB users with a probability of 100%, whereas for the URLLC the outage probability remains at acceptable levels.

VIII. Conclusion and Future Directions

In this work we studied the coexistence of URLLC and eMBB service on a Cf-maMIMO RAN. In particular, we devised a new theoretical model accounting for new assumptions related to network slicing applied to the Cf-maMIMO to multiplex heterogeneous services.

We introduced two customized procedures to assign pilot sequences to users, namely the Random PA and Greedy PA, where the latter has been defined with the purpose of minimizing the network slice pilot contamination. The results show that in the proposed configuration the PA choice does not influence the performance except in a low interference regime. Then we may conclude that the Cf-maMIMO architecture, relying by design on the macro-diversity gain offered by the

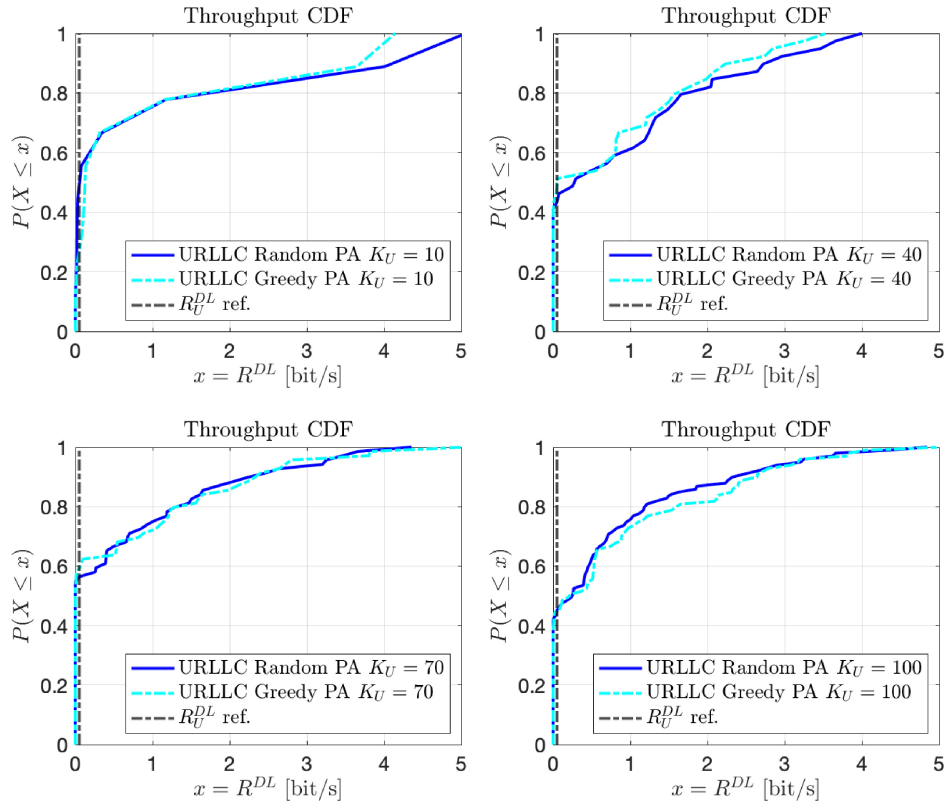

Fig. 6. CDFs of the URLLC throughput for different numbers of UEs for the two considered PAs.

distributed antennas, is able to fulfil the requirements for the considered heterogeneous services independently from the PA scheme.

Future directions of this work include the performance evaluation of the same system with different propagation conditions and different precoding techniques, also relaxing the assumption of the orthogonality between the two sets of pilot sequences. Finally, we plan to study alternative PAs, including implementations based on reinforcement learning algorithms, and will infer whether such schemes can allow us to relax the Cf-maMIMO condition $M >> K$ and get the number of APs closer or even below to the number of UEs.

APPENDIX
DERIVATION OF THE SE TERMS

In the following we report the detailed calculations of the terms S_u and $I_{u,e}$ of the closed-form expression (21) for the spectral efficiency. We remind that for a user i served by the m-th AP the channel estimation error is $\epsilon_{mi} = \hat{g}_{mi} - g_{mi}$, and, as in [27], the following conditions hold: $\mathrm{E}\{\epsilon_{mi}\hat{g}_{mi}\} = 0$ and $\mathrm{E}\{\epsilon_{mi}(\tilde{y}_{mi}^{(U)})^H\} = 0$. This is due to the fact that the channel estimation error ϵ_{mi} and the estimates $\hat{g}_{mi}$ are jointly Gaussian distributed, thus they are uncorrelated. For the S_u term in the SE expression we have:

$$|S_u|^2 = \left| \mathbb{E}\left\{ \sum_{m_u \in M_U} \sqrt{N_d^{(U)} \rho_{\mathrm{u}}} g_{m_u,u} \hat{g}_{m_u,u} \right\} \right|^2$$

$$= \left| \sqrt{N_d^{(U)} \rho_{\mathrm{u}}} \mathbb{E}\left\{ \sum_{m_u \in M_U} g_{m_u,u} \hat{g}_{m_u,u} \right\} \right|^2 . \quad (31)$$

By expressing $g_{m_u,u}$ in terms of the estimation error $\epsilon_{m_u,u}$, we have:

$$\mathbb{E}\left\{ \sum_{m_u \in M_U} g_{m_u,u} \hat{g}_{m_u,u} \right\} =$$

$$= \mathbb{E}\left\{ \sum_{m_u \in M_U} \left(\hat{g}_{m_u,u} - \epsilon_{m_u,u} \right) \hat{g}_{m_u,u} \right\} =$$

$$= \mathbb{E}\left\{ \sum_{m_u \in M_U} \left(\hat{g}_{m_u,u} \hat{g}_{m_u,u} - \epsilon_{m_u,u} \hat{g}_{m_u,u} \right) \right\} =$$

$$= \mathbb{E}\left\{ \sum_{m_u \in M_U} \left| \hat{g}_{m_u,u} \right|^2 - \sum_{m_u \in M_U} \epsilon_{m_u,u} \hat{g}_{m_u,u} \right\} =$$

$$= \sum_{m_u \in M_U} \mathbb{E}\left\{ \left| \hat{g}_{m_u,u} \right|^2 \right\} - \sum_{m_u \in M_U} \mathbb{E}\left\{ \epsilon_{m_u,u} \hat{g}_{m_u,u} \right\} \quad (32)$$

With the condition $\mathrm{E}\{\epsilon_{mi}\hat{g}_{mi}\} = 0$, we get

$$|S_u|^2 = \left| \sqrt{N_d^{(U)} \rho_{\mathrm{u}}} \sum_{m_u \in M_U} \gamma_{m_u,u} \right|^2 =$$

$$= N_d^{(U)} \rho_{\mathrm{u}} \left(\sum_{m_u \in M_U} \gamma_{m_u,u} \right)^2 \quad (33)$$

where $\gamma_{(m_u,u)}$ is defined in (15).

With the same considerations, we obtain the term $I_{u,e}$:

$$\mathbb{E}\{|I_{u,e}|^2\} = \left|\mathbb{E}\left\{\sum_{e\in K_E}\sum_{m_e\in M_E}\sqrt{N_d^{(E)}\rho_{\mathrm{e}}}g_{m_e,u}\hat{g}_{m_e,e}\right\}\right|^2 = \\ = \left|\sqrt{N_d^{(E)}\rho_{\mathrm{e}}}\mathbb{E}\left\{\sum_{e\in K_E}\sum_{m_e\in M_E}g_{m_e,u}\hat{g}_{m_e,e}\right\}\right|^2. \tag{34}$$

By expressing $g_{m_e,u}$ in terms of the estimation error $\epsilon_{m_e,u}$:

$$\mathbb{E}\left\{\sum_{e\in K_E}\sum_{m_e\in M_E}g_{m_e,u}\hat{g}_{m_e,e}\right\} = \\ = \mathbb{E}\left\{\sum_{e\in K_E}\sum_{m_e\in M_E}\left(\hat{g}_{m_e,u}-\epsilon_{m_e,u}\right)\hat{g}_{m_e,e}\right\}. \tag{35}$$

Defining

$$G_{\mathrm{UE}} = \mathbb{E}\left\{\sum_{e\in K_E}\sum_{m_e\in M_E}\hat{g}_{m_e,u}\hat{g}_{m_e,e}\right\} \tag{36}$$

and

$$C_{\epsilon\hat{g}} = \mathbb{E}\left\{\sum_{e\in K_E}\sum_{m_e\in M_E}\epsilon_{m_e,u}\hat{g}_{m_e,e}\right\}, \tag{37}$$

we have

$$|I_{u,e}|^2 = N_d^{(E)}\rho_{\mathrm{e}}\left|G_{\mathrm{UE}}-C_{\epsilon\hat{g}}\right|^2 = \\ = N_d^{(E)}\rho_{\mathrm{e}}\left(G_{\mathrm{UE}}^2+C_{\epsilon\hat{g}}^2-2G_{\mathrm{UE}}C_{\epsilon\hat{g}}\right). \tag{38}$$

With some algebra, we have:

$$G_{\mathrm{UE}}^2 = \sum_{e\in K_E}\sum_{m_e\in M_E}\mathbb{E}\left\{\left|\hat{g}_{(m_e,u)}\right|^2\right\}\mathbb{E}\left\{\left|\hat{g}_{m_e,e}\right|^2\right\} = \\ = \sum_{e\in K_E}\sum_{m_e\in M_E}\gamma_{m_e,u}\gamma_{m_e,e}, \tag{39}$$

$$C_{\epsilon\hat{g}}^2 = \sum_{e\in K_E}\sum_{m_e\in M_E}\mathbb{E}\left\{\left|\epsilon_{m_e,u}\right|^2\right\}\mathbb{E}\left\{\left|\hat{g}_{m_e,e}\right|^2\right\} = \\ = \sum_{e\in K_E}\sum_{m_e\in M_E}\left(\beta_{m_e,u}-\gamma_{m_e,u}\right)\gamma_{m_e,e}. \tag{40}$$

With the condition $\mathrm{E}\{\epsilon_{mi}\hat{g}_{mi}\}=0$, we get

$$G_{\mathrm{UE}}C_{\epsilon\hat{g}} = \\ = \sum_{e\in K_E}\sum_{m_e\in M_E}\mathbb{E}\{\epsilon_{m_e,u}\hat{g}_{m_e,u}\}\mathbb{E}\{\hat{g}_{m_e,e}\hat{g}_{m_e,e}\} = 0 \tag{41}$$

and (38) simplifies to

$$|I_{u,e}|^2 = N_d^{(E)}\rho_{\mathrm{e}}\sum_{e\in K_E}\sum_{m_e\in M_E}\left[\gamma_{m_e,e}\right. \\ \left.\cdot\left(\gamma_{m_e,u}+\beta_{m_e,u}-\gamma_{m_e,u}\right)\right] = \\ = N_d^{(E)}\rho_{\mathrm{e}}\sum_{e\in K_E}\sum_{m_e\in M_E}\gamma_{m_e,e}\beta_{m_e,u}. \tag{42}$$

REFERENCES

[1] M. Almekhlafi, M. A. Arfaoui, C. Assi, and A. Ghrayeb, "Joint resource and power allocation for URLLC-eMBB traffics multiplexing in 6G wireless networks," in *Proc. ICC 2021–IEEE Int. Conf. Commun.*, 2021, pp. 1–6.

[2] A. Karimi, K. I. Pedersen, N. H. Mahmood, G. Pocovi, and P. Mogensen, "Efficient low complexity packet scheduling algorithm for mixed URLLC and eMBB traffic in 5G," in *Proc. IEEE 89th Veh. Technol. Conf. (VTC2019-Spring)*, 2019, pp. 1–6.

[3] Y. Prathyusha and T.-L. Sheu, "Coordinated resource allocations for eMBB and URLLC in 5G communication networks," *IEEE Trans. Veh. Technol.*, vol. 71, no. 8, pp. 8717–8728, Aug. 2022.

[4] H. Q. Ngo, A. Ashikhmin, H. Yang, E. G. Larsson, and T. L. Marzetta, "Cell-free massive MIMO: Uniformly great service for everyone," in *Proc. IEEE 16th Int. Workshop Signal Process. Adv. Wireless Commun. (SPAWC)*, 2015, pp. 201–205.

[5] H. He, X. Yu, J. Zhang, S. Song, and K. B. Letaief, "Cell-free massive MIMO for 6G wireless communication networks," *J. Commun. Inf. Netw.*, vol. 6, no. 4, pp. 321–335, Dec. 2021.

[6] M. Bashar et al., "Uplink spectral and energy efficiency of cell-free massive MIMO with optimal uniform quantization," *IEEE Trans. Commun.*, vol. 69, no. 1, pp. 223–245, Jan. 2021.

[7] Z. H. Shaik, E. Björnson, and E. G. Larsson, "MMSE-optimal sequential processing for cell-free massive MIMO with radio stripes," *IEEE Trans. Commun.*, vol. 69, no. 11, pp. 7775–7789, Nov. 2021.

[8] L. Wang, J. Yuan, X. Jiang, J. Cui, and B. Zheng, "Dynamic resource scheduling strategy with QoE-aware for the coexistence of eMBB and URLLC traffic," in *Proc. 13th Int. Conf. Wireless Commun. Signal Process. (WCSP)*, 2021, pp. 1–5.

[9] M. Alsenwi, S. R. Pandey, Y. K. Tun, K. T. Kim, and C. S. Hong, "A chance constrained based formulation for dynamic multiplexing of eMBB-URLLC traffics in 5G new radio," in *Proc. 2019 Int. Conf. Inf. Netw. (ICOIN)*, 2019, pp. 108–113.

[10] T. Han and D. Zhao, "Energy efficiency of user-centric, cell-free massive MIMO-OFDM with instantaneous CSI," *Entropy*, vol. 24, no. 2, p. 234, 2022.

[11] M. Alsenwi, N. H. Tran, M. Bennis, A. Kumar Bairagi, and C. S. Hong, "eMBB-URLLC resource slicing: A risk-sensitive approach," *IEEE Commun. Lett.*, vol. 23, no. 4, pp. 740–743, Apr. 2019.

[12] S. Buzzi, C. D'Andrea, A. Zappone, and C. D'Elia, "User-centric 5G cellular networks: Resource allocation and comparison with the cell-free massive MIMO approach," *IEEE Trans. Wireless Commun.*, vol. 19, no. 2, pp. 1250–1264, Feb. 2020.

[13] K. Senel, E. Björnson, and E. G. Larsson, "Human and machine type communications can coexist in uplink massive MIMO systems," in *Proc. IEEE Int. Conf. Acoust., Speech Signal Process. (ICASSP)*, 2018, pp. 6613–6617.

[14] M. E. Alolaby, R. Dziyauddin, and L. A. Latiff, "Reduction of HARQ latency for URLLC 5G services based on network slicing and massive MIMO hybrid beamforming," *Int. J. Integr. Eng.*, vol. 12, no. 7, pp. 28–39, 2020.

[15] V. Jumba, S. Parsaeefard, M. Derakhshani, and T. Le-Ngoc, "Resource provisioning in wireless virtualized networks via massive-MIMO," *IEEE Wireless Commun. Lett.*, vol. 4, no. 3, pp. 237–240, Jun. 2015.

[16] P. Parida and H. S. Dhillon, "Pilot assignment schemes for cell-free massive MIMO systems," 2021, *arXiv:2105.09505*.

[17] S. Buzzi, C. D'Andrea, M. Fresia, Y.-P. Zhang, and S. Feng, "Pilot assignment in cell-free massive MIMO based on the Hungarian algorithm," *IEEE Wireless Commun. Lett.*, vol. 10, no. 1, pp. 34–37, Jan. 2021.

[18] Y. Zhang, H. Cao, P. Zhong, C. Qi, and L. Yang, "Location-based greedy pilot assignment for cell-free massive MIMO systems," in *Proc. IEEE 4th Int. Conf. Comput. Commun. (ICCC)*, 2018, pp. 392–396.

[19] M. Attarifar, A. Abbasfar, and A. Lozano, "Random vs structured pilot assignment in cell-free massive MIMO wireless networks," in *Proc. IEEE Int. Conf. Commun. Workshops (ICC Workshops)*, 2018, pp. 1–6.

[20] A.-S. Bana et al., "Massive MIMO for Internet of Things (IoT) connectivity," 2019, *arXiv:1905.06205*.

[21] Y.-H. Hsu and W. Liao, "eMBB and URLLC service multiplexing based on deep reinforcement learning in 5G and beyond," in *Proc. IEEE Wireless Commun. Netw. Conf. (WCNC)*, 2022, pp. 1467–1472.

[22] A. K. Bairagi et al., "Coexistence mechanism between eMBB and URLLC in 5G wireless networks," *IEEE Trans. Commun.*, vol. 69, no. 3, pp. 1736–1749, Mar. 2021.

[23] M. Alsenwi, N. H. Tran, M. Bennis, S. R. Pandey, A. K. Bairagi, and C. S. Hong, "Intelligent resource slicing for eMBB and URLLC coexistence in 5G and beyond: A deep reinforcement learning based approach," *IEEE Trans. Wireless Commun.*, vol. 20, no. 7, pp. 4585–4600, Jul. 2021.
[24] E. Björnson, J. Hoydis, and L. Sanguinetti, "Massive MIMO networks: Spectral, energy, and hardware efficiency," *Found. Trends Signal Process.*, vol. 11, nos. 3–4, pp. 154–655, 2017.
[25] Ö. T. Demir, E. Björnson, and L. Sanguinetti, "Foundations of user-centric cell-free massive MIMO," *Found. Trends Signal Process.*, vol. 14, nos. 3-4, pp. 162–472, 2021.
[26] H. Q. Ngo, A. Ashikhmin, H. Yang, E. G. Larsson, and T. L. Marzetta, "Cell-free massive MIMO versus small cells," *IEEE Trans. Wireless Commun.*, vol. 16, no. 3, pp. 1834–1850, Mar. 2017.
[27] T. L. Marzetta, E. G. Larsson, H. Yang, and H. Q. Ngo, *Fundamentals of Massive MIMO*. Cambridge, U.K.: Cambridge University Press, 2016.
[28] J. Qiu, K. Xu, Z. Shen, W. Xie, D. Zhang, and X. Li, "Downlink performance analysis of cell-free massive MIMO over spatially correlated Rayleigh channels," in *Proc. IEEE 19th Int. Conf. Communication Technol. (ICCT)*, 2019, pp. 122–127.
[29] *Further Advancements for E-UTRA Physical Layer Aspects, Release 9*, 3GPP Standard TR 36.814, 2010.

Ubaldo Bucci (Student Member, IEEE) received the bachelor's degree in 2014, the master's degree in 2018, and the Ph.D. degree in "engineering and information science" curriculum: new computational models: algorithms, software architectures, intelligent system in January 2023. He started its educational path in computer science in 2009. He is currently working as an Integration and Verification Engineer with the Nokia's Research and Development Department, Nokia, Athens.

Dajana Cassioli (Senior Member, IEEE) is an Associate Professor of Telecommunications Engineering with the University of L'Aquila, Italy. Since 2015, she has been the Coordinator of the University of L'Aquila Node of the CINI National Laboratory of Cybersecurity, where she led the CyberEquality WG from 2020 to 2021. She was the CEO of the spin-off of the University of L'Aquila "Smartly: Natives of Smart Living srl" from 2014 to 2018 and in 2019. She was a Summer Manager with the Wireless Systems Research Department, AT&T Labs-Research, NJ, USA, in 2000. She was a Visiting Short-Term Scholar with the University of Southern California, LA, USA, in 2022. She participated in the definition of the standard channel model for the IEEE 802.15.4 standard in 2005. Her main research interests are in wireless communications, 5G/B5G networks, and cybersecurity. She is the Chair of the IEEE ComSoc RCC SiG on Propagation Channels for 5G&B and the Diversity, Equity and Inclusion Activity Coordinator of the IEEE Italy Section. She is the Past Chair of IEEE WIE AG Italy Section from 2016 to 2022 and IEEE VT06/COM19 Italy Chapter from 2011 to 2017. She has been awarded the ERC StG VISION (Video-oriented UWB-based Intelligent Ubiquitous Sensing) in 2010 and the ERC PoC Grant iCARE (MobIle health-Care system for monitoring toxicity and symptoms in cAncer patients Receiving diseasE-oriented therapy) in 2016. She served as the IEEE EUROCON 2023 WIE Chair, the IEEE ICC 2023 CISS Co-Chair, the PIMRC2018 Industry Co-Chair, the RTSI WIE Chair in 2018, 2019, and 2020, MELECON2020, and MetroInd4.0, and a TPC Member of several International Conferences (ICC, PIMRC, VTC, and GLOBECOM). She is an Associate Editor of *IET Electronics Letters* and IEEE COMMUNICATIONS LETTERS and an Executive Editor of *Internet Technology Letters* (Wiley) and *Transactions on Emerging Telecommunications Technologies* (Wiley).

Andrea Marotta (Member, IEEE) received the M.Sc. degree in computer engineering and the Ph.D. degree in information and communications technology from the University of L'Aquila, Italy, in 2015 and 2019, respectively,

He is an Assistant Professor with the Department of Information Engineering, Computer Science and Mathematics, University of L'Aquila. He was a Visiting Researcher with the Group for Research on Wireless, Instituto Superior Técnico/University of Lisbon, with the Research Institute of Communication, Information and Perception Technologies, Scuola superiore di studi universitari e di perfezionamento Sant'Anna, Pisa, and with the Computer Networks Lab, University of California at Davis, Davis. He performs research on network reliability, SDM optical networks, multi-access edge computing, 5G software defined access, and CoMP coordinated scheduling. He actively participates in the TPC of IEEE Communications Society conferences.

Open Access funding provided by 'Università degli Studi dell'Aquila' within the CRUI CARE Agreement